PHYSICAL REVIEW A VOLUME 36, NUMBER 6 SEPTEMBER 15, 1987

Time-dependent Hartree-Fock theory of multiphoton ionization: Helium

Kenneth C. Kulander
Theoretical Atomic and Molecular Physics Group, Lawrence Livermore National Laboratory, Livermore, California 94550
(Received 16 March 1987)

The multiphoton ionization of helium has been determined for a number of laser wavelengths and intensities using the time-dependent Hartree-Fock model. Conclusions about the ionization dynamics for very-short-pulse, high-intensity lasers are discussed. The limits and characteristics of the time-dependent Hartree-Fock method for atomic physics processes are also evaluated.

I. INTRODUCTION

The study of multiphoton ionization of atoms has experienced intense interest over the past few years due to exciting new experimental results obtained with short-pulse, high-power lasers. Most interesting are the observations of a spectrum of photoelectron energies indicating the absorption of a large number of excess photons during ionization[1-3] [above-threshold ionization (ATI)] and the production of very high ionization stages.[4-6] The probability of multiply ionizing atoms was found to be surprisingly large relative to the single-ionization yield leading to speculation that some sort of collective modes of the atoms were being excited.

Traditional perturbation theory (PT) has been capable of treating most of the observed data so far,[7,8] but it is clear that more intense shorter-pulsed lasers will push the multiphoton ionization process into the regime where PT breaks down. It is one intention of the research reported here to explore the limits of PT and to predict the behavior of atoms in fields with intensities and pulse shapes beyond those for which PT is valid.

The response of a multielectron atom to a very strong field (generally corresponding to intensities in excess in 10^{14} W/cm^2) can be predicted reliably only using a time-dependent approach. For short, intense pulses, the ionization rate can be fast on the time scale of the oscillations of the field. Under these circumstances the assumption of a monochromatic field is incorrect. For laser intensities above 10^{16} W/cm^2, the electric field becomes stronger than the interelectronic interactions. This also causes the breakdown of PT based on treating the laser as a perturbation. By explicit integration of the time-dependent Schrödinger equation, the effects of the pulse shape (rise time) and high intensity can be treated exactly. Whereas this is feasible for a single-electron atom,[9] the equations are intractable for multielectron systems.

A method which has been used successfully for strong collisions of multielectron atoms is the time-dependent Hartree-Fock (TDHF) or time-dependent self-consistent-field method.[10-12] In this approach the time evolution of the electronic orbitals is followed using the mean field of the total electron density as part of a time-dependent potential. In this way some of the instantaneous correlation of the electrons is smeared out or averaged over, while the rest of the interactions, the nuclear attractions, etc., are handled accurately. This mean-field approximation reduces the dimensionality of the problem significantly, from $3N$ particle coordinates to three spatial dimensions for N orbitals, so that manageable calculations can be performed.

Using this approach, we have performed a number of calculations for the two-electron helium atom. The results can, with caution, be extrapolated to systems with more electrons. These calculations explore the effects of pulse shape, peak intensity, and wavelength on the preionization dynamics (PD) of the electrons in the atom. We also obtain ionization rates for constant-intensity interactions when an exponential decay of the initial state is observed. These calculations show that ionization rates which are indeed fast compared to the laser oscillation rate are predicted for intensities realizable in the laboratory.

They also show that the PD can change dramatically for different wavelengths. At very short wavelengths there is evidence that a collective mode could be excited and play an important role in the PD. If this is the case, some prospect exists of producing very highly excited states of the atom, well above the ionization potential, for times comparable to autoionization lifetimes. It is difficult to imagine constructing such "collective" states for multielectron systems in a basis-set-type calculation. If these states are not included in the calculations, we cannot find out whether they play a role in the PD. Therefore, our approach is to use numerical orbitals, which require no preconceived notions about their form, and only limited assumptions about their extent. In this way we attempt to allow the laser interaction and the time-dependent mean field to drive the evolution of the system without limits. This is achieved in part in these calculations, but not entirely. As discussed below, we place the restriction on the wave function that it can be represented, for all time, by a single Slater determinant. This constraint inhibits proper autoionization and treats the state of the system in an averaged sense rather than in terms of quantum states with specific amplitudes. The physical meaning of this constraint and the interpretation of the results are also the subjects of this investigation. The tractability of the TDHF method to treat complicated processes makes it attractive for development. But, since it is a relatively new method in atomic

physics, its applicability and limitations are yet to be completely understood.

In Sec. II we will present in some detail the method of calculation used in studying multiphoton ionization of helium. In Sec. III we will present many results of both the PD and the ionization rates for various intensities and frequencies. Section IV contains our conclusions about both the multiphoton ionization dynamics and the method itself.

II. METHOD

Calculations of the multiphoton ionization of helium have been carried out in two approximations which illustrate or emphasize different aspects of the possible ionization dynamics. In the first calculation, the helium system is treated as a one-electron atom by freezing one of the electrons in its ground-state (static Hartree-Fock) orbital. In this case, the active electron absorbs energy from the laser field in the potential given by the nuclear attraction and the mean Coulomb field of the frozen second electron. Of course, there is no mechanism in this calculation for the excited electron to share its energy with the other electron. The second calculation is carried out using the method commonly described as the time-dependent Hartree-Fock or the time-dependent self-consistent-field technique. In this calculation the electronic wave function is given by a single Slater determinant, whose time evolution is given in terms of the evolution of the individual orbitals. In the case of helium, the wave function is given by a single, doubly occupied atomic orbital which evolves in time in response to the laser field, the nuclear attraction, and the time-dependent mean field due to the Coulomb interaction between the electrons. The basic difference between the two calculations is that the second case allows the electrons to share the absorbed energy, albeit in a constrained way, so the possibility of collective effects can be examined.

We explicitly solve the mean-field approximation to the time-dependent Schrödinger equation:

$$i\hbar\frac{\partial}{\partial t}\psi(\mathbf{r},t)=H(\mathbf{r},t)\psi(\mathbf{r},t)\ , \tag{1}$$

where the time dependence in the Hamiltonian comes from the photon-electron interaction. The wavelengths of interest are large compared to the size of the atom so that the dipole approximation is valid. The matter-radiation interaction term, assuming a classical field, is given by

$$V_I=-eE(t)z\sin(\omega t) \tag{2}$$

where we assume a linearly polarized laser field.

The general form of the TDHF solution of Eq. (1) assumes a completely antisymmetrized product wave function

$$\psi(\mathbf{r}_1\cdots\mathbf{r}_n,t)=A\prod_{i=1}^{n}\phi_i(\mathbf{r}_i,t)\ . \tag{3}$$

Putting Eq. (3) into Eq. (1) and taking moments with the presumed orthonormal orbitals, we obtain the usual TDHF equation,

$$i\frac{\partial}{\partial t}\phi_i=(h+V_I)\phi_i,\quad i=1,\ldots,n \tag{4}$$

where the Fock operator, h, is given by

$$h\phi_i(\mathbf{r})=-(\hbar^2/2m)\nabla^2+e^2\sum_j\int d\mathbf{r}'\,|\phi_j(\mathbf{r}')|^2/|\mathbf{r}-\mathbf{r}'|-Ze^2/r-e^2\sum_{j>i}'\left[\int d\mathbf{r}'\,\phi_j(\mathbf{r}')\phi_i(\mathbf{r}')/|\mathbf{r}-\mathbf{r}'|\right]\phi_j(\mathbf{r})\ . \tag{5}$$

The TDHF method is an initial value problem, for which the initial conditions are chosen to be the ground, static Hartree-Fock wave function of the system. At time $t=0$, the interaction term, Eq. (2), is zero with our choice of phase. The envelop function $E(t)$ is normally chosen to rise linearly over five to ten oscillation periods, then be constant thereafter. During the constant interval, an ionization rate can be determined if the decay is found to be exponential. For helium, the initial state is a singlet so that there is a single spatial orbital and no exchange term in the Fock operator.

We solve this partial differential equation using a finite-difference representation of the electronic wave function. (See Ref. 11 and references therein for details.) The Hamiltonian for an atom in a linearly polarized laser field has cylindrical symmetry. For an s orbital, we can write

$$\phi(\mathbf{r},t)=\rho^{-1/2}\chi(\rho,z,t) \tag{6}$$

and set up a two-dimensional grid in ρz space defined by

$$\rho_j=\Delta(i-1/2),\quad j=1,\ldots,nr \tag{7}$$

and

$$z_k=\Delta[k-(nz+1)/2],\quad k=1,\ldots,nz \tag{8}$$

with equal grid spacing Δ in both dimensions. Putting Eq. (6) into Eq. (4), we obtain a set of coupled finite-difference equations for the values of the orbital at the grid points. The prefactor in the definition in Eq. (6) removes the first derivative term in the radial direction in the cylindrical Laplacian. Then the kinetic energy is calculated using a three-point difference formula. These difference equations are derived variationally after the discretization has been made.[13]

The time propagation is accomplished using a Peaceman-Rachford, alternating directions implicit method which has been used and described previously for TDHF calculations.[11,13] The advantage of this particular propagator is that it is stable, unitary, and requires only vector multiplication and tridiagonal matrix inversion. Both of these manipulations are linear in the number of grid points and are easily vectorized. In fact, we find that on a vector machine, the computation time

increases more slowly than the number of grid points. In particular, doubling the number of points in each dimension resulted in the overall calculation time increasing by a factor of 3.4. The integration parameters (grid spacing, grid size, time step, etc.) have been varied to determine the sensitivity of the results we report. The calculated ionization rates changed by less than 20% for reasonable variations of the parameters. The grid spacing was typically chosen to be $0.2a_0$ and the time step such that it required 200–400 steps per oscillation period of the field. The stability of the evolution is evidenced by constant ionization rates over thousands of integration steps during the constant intensity period of the calculations.

The calculation proceeds as follows. The static Hartree-Fock ground-state wave function is determined by propagating an approximate ground state in imaginary time. The wave function relaxes to the true ground state for the finite grid in 20–50 integration steps. This initial state is then propagated in real time according to Eq. (4). The amplitude of the field, $E(t)$, rises linearly over an integral number of cycles, then is held constant. The number of cycles chosen for the turn on interval generally is large enough that the increase is approximately adiabatic. The wavelengths we have considered are well off resonance so that we find no significant effects due to the length of the turn-on period. During the propagation, the time-dependent wave function is projected onto the initial state, and excited states, in order to identify the dynamics of the excitation process. Also, since the grid has finite extent, we include an absorbing interaction on the boundary. The range and strength of this imaginary potential is chosen so that minimal reflection of the wave function occurs. The distance to the boundary is chosen large enough that the predicted ionization rates are not affected. This is possible because once the electron is far from the nucleus, it can no longer absorb or emit photons: it is very unlikely that the electron will be turned around by the field once it has reached the boundary. An exception to this occurs for the long-wavelength, high-intensity cases for which reflection from a ponderomotive barrier[14–16] may occur. We generally perform the projections onto bound-state wave functions only at times when $\omega t = n\pi$.

As we found in our hydrogen calculations,[9] for direct ionization, the ionization rates determined either by the disappearance of the ground-state probability or the decrease in the norm of the wave function due to the absorption at the boundary, are identical. If the ionization is indirect, proceeding through bound or quasibound intermediates, we find Rabi oscillations in the ground-state population and generally, nonexponential decay of the norm. The consequences of this sort of PD, both in terms of ionization rates and the TDHF model itself, are discussed below.

III. RESULTS

Before discussing the ionization rates and results, some discussion of TDHF is appropriate. In the short time limit, TDHF is equivalent to the random-phase approximation (RPA) or random-phase-approximation with exchange (RPAE) which can give reasonable excitation and ionization cross sections. For long-time propagation which we employ here, we consider the evolution of the wave function to represent an average-atom picture of the process. Helium is a good starting point for understanding the characteristics of the time-evolving wave function. The doubly occupied orbital can be expressed as a linear combination of atomic orbitals

$$\phi(t) = a_{1s}(t)\phi_{1s} + a_{2s}(t)\phi_{2s} + a_{2p}(t)\phi_{2p} + \cdots . \quad (9)$$

Initially, of course, a_{1s} is one with the rest of the time-dependent expansion coefficients being zero. Putting two electrons in this time-dependent orbital with opposite spins, we have the wave function expressed in terms of zero-order singly and doubly excited (singlet) product states of the system. Of course, the continuum states must also be included in this expansion.

This expansion illustrates two defects of the TDHF wave function. First, the single-configuration wave function forces, for example, the amplitude in the $1s2p$ state to be related to that for the $2p^2$ state. Second, these product states are not accurate representations of the true excited states. Since the TDHF equations are nonlinear in the orbitals, the principle of superposition, which is valid for the Schrödinger equation, does not hold. For these reasons, the TDHF wave function is best interpreted as an *averaged* representation of the exact wave function. This means that it is averaged in the sense of a multiconfiguration solution of a time-dependent Schrödinger equation which evolves in an average field. For systems with a very high density of states, a mean-field theory generally gives a good approximation to the system's dynamics. For multielectron atoms, this should be the case. But for helium, which has a very low density of states, with no bound doubly excited states, this approximation is severe.

Finally, the single-configuration restriction inhibits the autoionization of doubly excited states. It does not exclude it entirely, but the autoionization rate will be greatly underestimated. Making allowances for inaccurate excitation energies and hindered autoionization, much can be learned about the behavior of atoms in intense fields using this approach.

We first discuss in detail the results for the long-wavelength, multiphoton ionization of He for a particular wavelength, 1.064 μm, and peak intensity, 1×10^{15} W/cm^2. We emphasize this case in order to illustrate some of the information which can be obtained in a single calculation.

As stated above, the initial state is chosen to be the ground, static Hartree-Fock wave function of the finite-difference Hamiltonian. This is determined by propagation of an approximate ground state in imaginary time until the expectation value of the total energy converges. We have used a grid with 259 points in the z direction and 100 points in the ρ direction with a grid spacing of $0.2a_0$. We obtain an initial state energy of -75.95 eV, which compares well with the Hartree-Fock limit of -77.87 eV. The respective orbital energies are -24.28 and -24.98 eV. The true ionization potential is 24.58 eV and the total energy is -78.98 eV. The main error

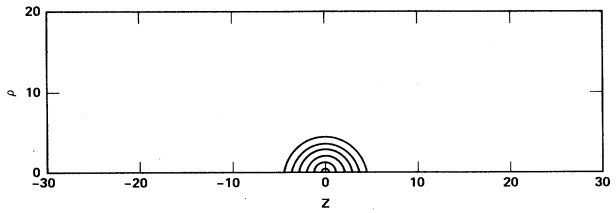

FIG. 1. Density plot of the initial helium orbital. Contours differ by a factor of 10.

in these numbers comes from the sparse representation of the wave function near the nucleus. The evaluation of the nuclear attraction on this grid, therefore, is the least accurate term in the total energy. We assume this is not serious with respect to calculations of multiphoton ionization. Because of the error in the ionization potential, the number of photons required to ionize the atom differs by one (22 versus 21) for the 1.064-μm case with respect to the Hartree-Fock (Koopmans's) or the true ionization potentials. This is not terribly important because the ionization process, in these long-wavelength cases with the intensities considered in this work, is in the Keldysh or tunneling regime and does not depend very strongly on the wavelength.[17,18] This will be discussed further below.

First we show in Fig. 1 the initial-state wave function. The density contours differ by an order of magnitude so that the outer contour represents a density 10^{-5} of the peak density. The figure also shows the approximate size of the grid used in the calculations. The true boundaries are at $z=\pm 25.8a_0$ and $\rho=20.1a_0$. We consider a calculation for the field defined in Eq. (2) where $E(t)=E_{\max}f(t)$ and

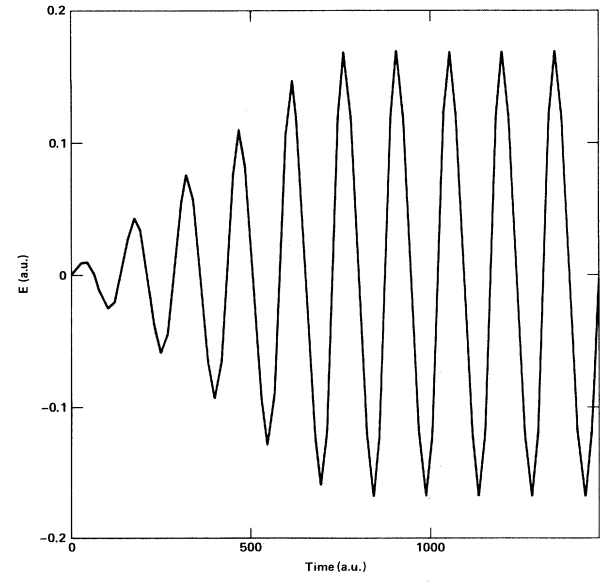

FIG. 2. Time evolution of the classical field strength for a photon wavelength of 1.064 μm and a rise time of five periods. Time is in atomic units (2.4189×10^{-17} s).

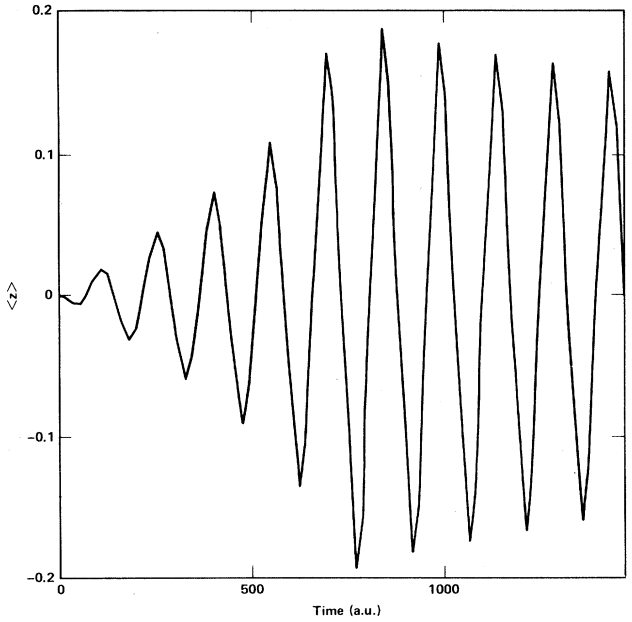

FIG. 3. Time-dependent expectation value of z (in atomic units).

$$f(t)=\begin{cases} t/t_{\max}, & t<t_{\max} \\ 1, & t\geq t_{\max}\ . \end{cases} \tag{10}$$

Here $E_{\max}=0.169$ a.u. corresponding to the maximum laser intensity of 1×10^{15} W/cm^2 and $t_{\max}$ is chosen to be five oscillation periods of the field ($\omega t_{\max}=10\pi$). For photons with a 1.064-μm wavelength, the period is 3.55×10^{-15} s (147 a.u.). The calculations we discuss follow the evolution of the wave function for ten periods. Figure 2 shows the time dependence of the classical field for this calculation. During the first five periods the field increases linearly then is constant. In Figs. 3–5 we plot the time-dependent expectation values of z, z^2, ρ, and ρ^2. These all follow closely the time evolution of the field. As expected, the extent of the oscillations in the direction of polarization of the field are much smaller than for a free electron.[16] We note that the expectation values were determined every eighth of a period so that the curves are less smooth than they should be. It is important to note that the wave function does experience a periodic distortion, due to the oscillating field. This type of driven motion has been proposed as a mechanism for exciting the inner shell of a many-electron atom by the oscillations of the outer shell.[19] For larger systems, these calculations can show the extent of the motion of the least strongly bound shell and can be used to assess the extent to which laser energy can be coupled into the inner electrons through this mechanism. Note that this distortion corresponds to the *simultaneous* excitation of all the electrons in a given shell which may be difficult to represent accurately in a basis-set calculation. A Floquet calculation of the dressed state of a multielectron atom using a basis containing only single and double excitations from the initial configuration would be inade-

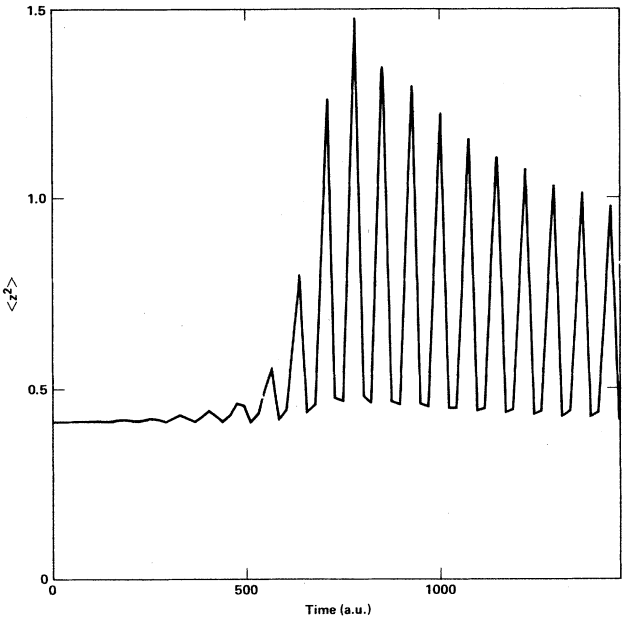

FIG. 4. Time-dependent expectation value of z^2.

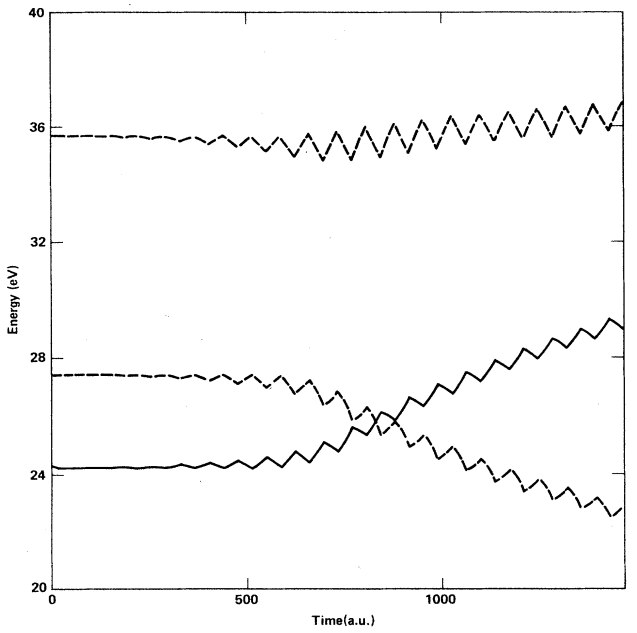

FIG. 6. Time-dependent expectation values of the single-particle kinetic energy (upper dashed line), the Coulomb repulsion (lower dashed line), and the negative of the orbital energy (solid line). Energies are in electron volts.

quate to describe this motion. With numerical orbitals, these multiply excited configurations are included automatically.

We also have determined the time evolution of the various contributions to the total energy. These are shown in Figs. 6 and 7. We define an expectation value of an operator $\hat{A}$ by

$$\langle \hat{A} \rangle = \langle \phi \mid \hat{A} \mid \phi \rangle / \langle \phi \mid \phi \rangle \tag{11}$$

to allow for the time-decreasing norm of the wave function due to the absorbing boundaries. This decay means the Coulomb integral, the second term on the right-hand

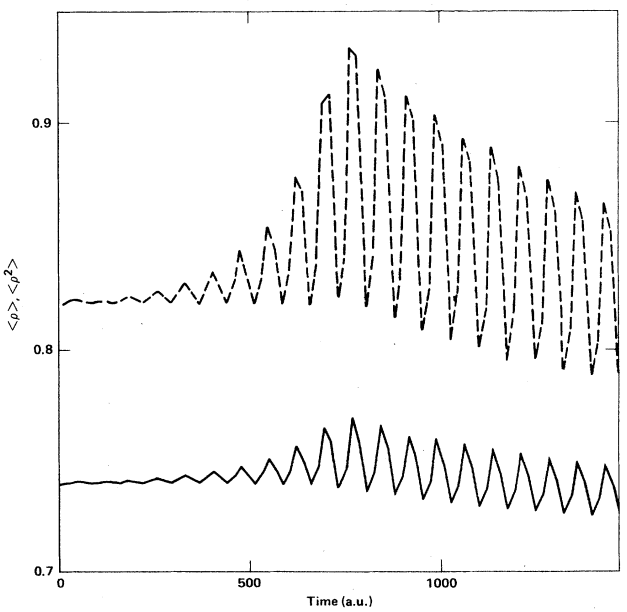

FIG. 5. Time-dependent expectation values of ρ and ρ^2 (solid line).

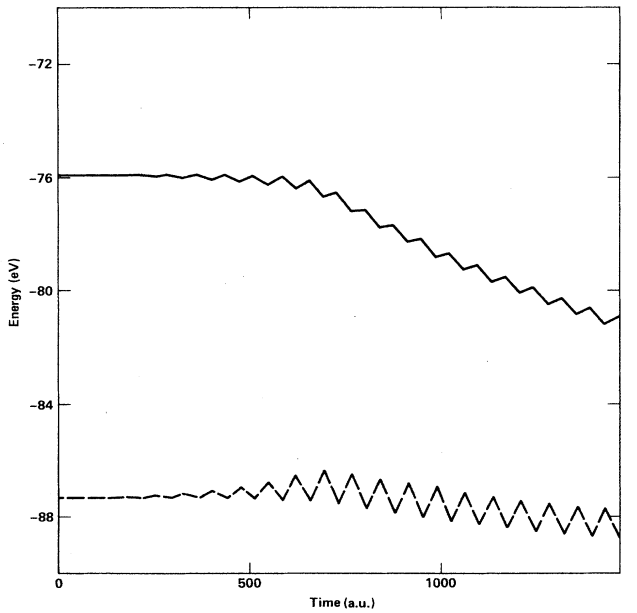

FIG. 7. Time-dependent expectation value of the nuclear attraction (dashed line) and the total electronic energy (solid line).

side of Eq. (5), gets weaker as the atom ionizes, as can be seen in Fig. 6. As the interelectronic repulsion becomes weaker, the orbital energy and the total energy both increase in magnitude, making it more difficult for the atom to ionize. This is a true many-electron effect in that we know the ionization potential for each stage of ionization of an atom is higher than the previous one. It is a characteristic of the TDHF method that this change is made in a continuous manner rather than in steps as would occur in a real atom. Note that from Figs. 6 and 7 we find that the nuclear attraction and kinetic energy change much more slowly than the Coulomb repulsion. This is due to the latter depending on the total electronic density, while the others do not. The oscillatory structure in all these expectation values follow the oscillations in the laser field. Also, the peak amplitudes of the expectation values of the size of the orbital shown in Figs. 3–5 decrease with time because of the orbital becoming more strongly bound.

We determine the extent to which the atom is excited by projecting the time-dependent wave function onto the initial state. In Fig. 8 we show both the time-dependent norm of the wave function and the probability remaining in the ground state. This projection onto the initial wave function may make physical sense only when the phase of the field is such that $\sin(\omega t)$ vanishes. In general, the projection should be onto dressed atomic states. However, to illustrate the variation of the wave function with time, we have projected onto the field-free ground state several times during each period to obtain the dashed line shown in Fig. 8. It is clear that only a small fraction of the wave function is excited from the ground state directly to the continuum during each period. This excited flux then propagates to the boundary of the grid and is absorbed. The flat segments in the time-dependent norm are due to the finite travel time for the electron to reach the boundary. The corresponding time interval indicates the electron energy is on the order of several electron volts, indicating a high probability of the electron having absorbed more than the minimum number of photons for ionization (ATI). A more quantitative analysis of the outgoing electron flux would be required to establish that this is indeed the fact, but experimentally this certainly has been found to be the case.

The decay of the initial state shown in Fig. 8 is found to be nonexponential during the last half of the integration time when the intensity is constant. This is due to the gradual increase in the binding energy, making ionization more difficult. Therefore, we find the ionization rate decreases as the ionization proceeds.

Such calculations give a reasonable understanding of the multiphoton ionization of helium in this long-wavelength limit. The ionization is predicted to be direct; no structure due to the excited states of the system is in evidence. By direct we mean the lack of appreciable excitation of any intermediate state as indirect photodissociation. We are not addressing the direct versus sequential emission of many electrons. We obtain further insight into the ionization dynamics from the time-dependent wave function itself. In Fig. 9, eight density plots of the time-dependent wave function during

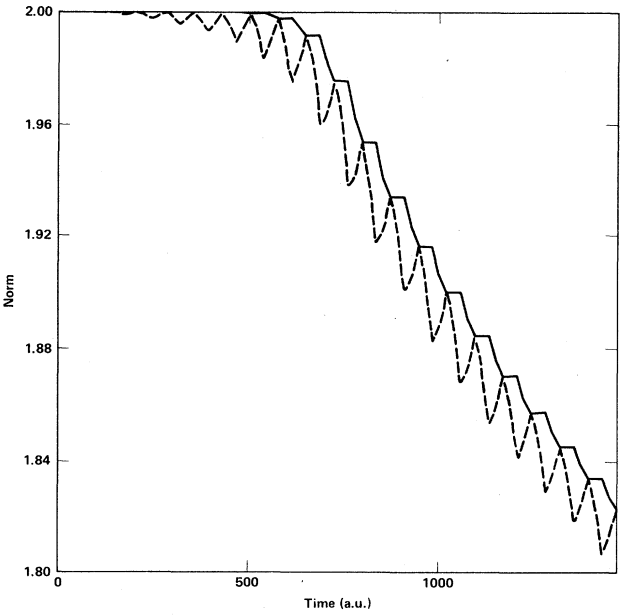

FIG. 8. Time evolution of the norm of the wave function (solid line) and the projection of the time-dependent wave function onto the ground (initial) state.

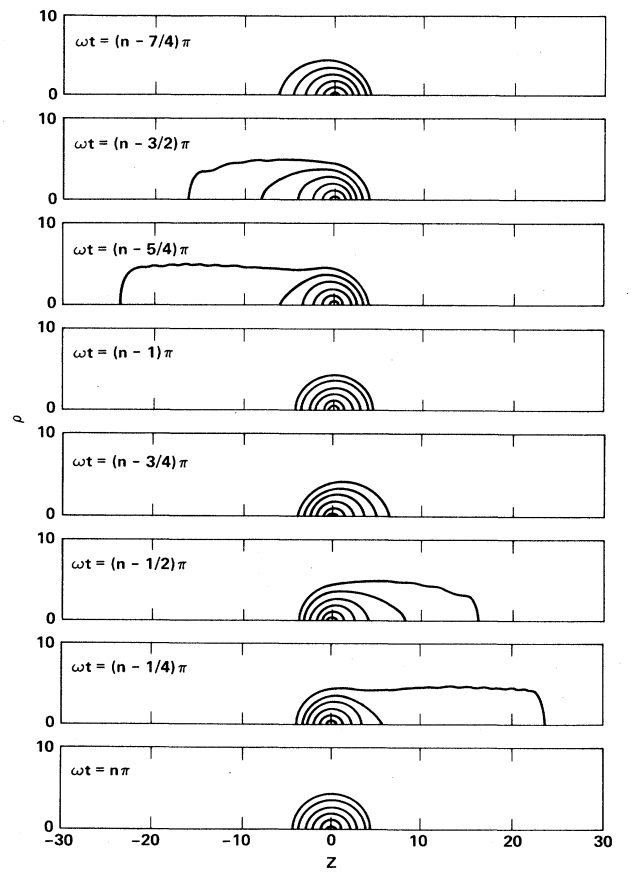

FIG. 9. Snapshots of the 21 + photon ionization of He at $I = 10^{15}$ W/cm^2.

one cycle are displayed. These show that the electrons emitted are strongly focussed along the direction of polarization. One might be concerned that the finite size of the grid could inhibit the excitation to a highly excited Rydberg state. We believe this does not prevent us from determining accurate ionization rates because this field is expected to ionize any Rydberg state very rapidly on the time scale of the excitation of the ground state.

At the highest intensities and longest wavelength considered, we observe the ionization flux emitted toward either the positive or negative z axis depending on the phase of the field as shown in Fig. 9. In these cases a free electron in the laser field would exhibit oscillations which are large compared to the size of the atom.[14–16] The maximum excursion of a free electron is given by

$$z_{\max}=\frac{eE}{m\omega^2}\ , \tag{12}$$

which for the worst case considered in Table I is approximately $130a_0$. This is much larger than our grid so that our absorbing boundary is inside the ponderomotive barrier whose height is given by

$$E_p=\frac{e^2E^2}{4m\omega^2}\ . \tag{13}$$

For the 1.064-μm laser at an intensity of 2×10^{15} W/cm^2 this barrier is greater than 200 eV. This means the electron must absorb an additional 200 eV above the field-free ionization potential in order to escape from the vicinity of the ion. It seems likely that once the electron has absorbed enough energy to be above the ionization potential, it will rapidly absorb more energy to climb out of the ponderomotive well. Having too small a grid to test this hypothesis means that our ionization rates for the highest intensity, longest-wavelength cases may be too high. Unfortunately, it requires an intractably large grid to test this hypothesis for the case described above. We did examine the 532-nm, 1×10^{15}-W/cm^2 case more closely. In this case the $z_{\max}$ is $23a_0$ so that our standard choice of boundary at $\pm26a_0$ might be inadequate to allow for reflections off of the ponderomotive barrier. Therefore, we performed a second calculation with the z boundaries at $\pm52a_0$ and found that the final ionization rate did in fact decrease by 15%. In this case the ponderomotive barrier is 26.4 eV. On the expanded grid, there appears to be some reflection of electron density from the ponderomotive barrier which, when it rescatters off the atom, may be deexcited back to the ground state. Also there is a much larger time delay between the disappearance of the ground-state probability and its absorption at the boundary. Because it only makes physical sense to project onto the initial, undressed state when the oscillating field vanishes, it is not possible to determine directly whether some probability is excited then deexcited during part of a period. We postulate this as an explanation for the lower rate of depletion of the ground state in the larger grid calculation. These conclusions are preliminary but indicate the first evidence of the role of the ponderomotive effect in a calculation of multiphoton ionization. A systematic study of this in a full three-dimensional system is computationally intractable. It should be possible to do so in a one-dimensional model, however.

For comparison with this high-order ionization process we show the excited wave function for the one- and two-photon ionization of helium in Fig. 10. These density plots obviously show the p and d character of the final continuum orbitals. Also, these cases differ significantly from the long-wavelength case in which ionization flux is first emitted to the right then to the left along the z axis during the period of the laser oscillation. In the low-order process the p- and d-wave character is the same throughout the whole period. We believe the long-wavelength behavior is consistent with the Keldysh-type tunneling model.[17] Our calculated one- and two-photon cross sections agree very well with perturbation results, illustrating the accuracy of this approach (see Table I).

As indicated above, we have also performed calculations using a single-electron model in which one of the 1s electrons is frozen in its initial orbital. The second electron interacts with the laser and moves in the

TABLE I. (a) Helium ionization rates (s^{-1}) and (b) (generalized) cross sections as functions of photon energy and laser intensity.

(a)

I (W/cm^2) \ wavelength (μm)	1.064		0.532	
	$1s^2$	$1s1s'$	$1s^2$	$1s1s'$
5×10^{14}	4.7×10^{11}	7.1×10^{11}	9.0×10^{11}	1.4×10^{12}
1×10^{15}	1.5×10^{13}	2.1×10^{13}	1.9×10^{13}	2.8×10^{13}
2×10^{15}	1.2×10^{14}	2.6×10^{14}	1.4×10^{14}	2.7×10^{14}
	9.0 eV			
1×10^{15}	2.6×10^{13}	5.8×10^{13}		

(b)

	TDHF	PT		$\hbar\omega$ (eV)
σ (cm^4/W^2 s)	3×10^{-16}	2.5×10^{-16}	(Refs. 25–27)	13.6
σ (cm^4/W^2 s)	1×10^{-16}	1.1×10^{-16}	(Refs. 25–27)	17.7
σ (cm^2)	4×10^{-18}	5×10^{-18}	(Refs. 28)	30.0

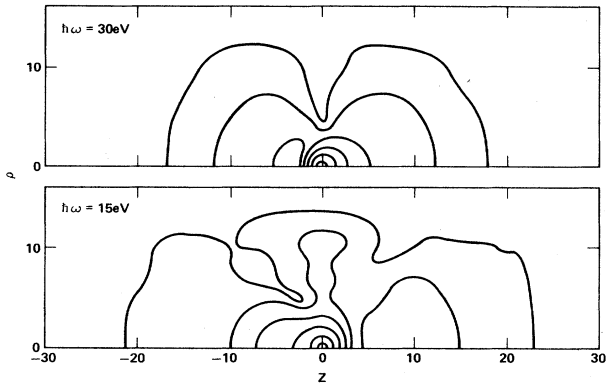

FIG. 10. Ionizing wave function for 30- and 15-eV photons.

Coulomb mean field of the frozen electron. In this way, we investigate several aspects of the ionization process. These calculations show that for the long-wavelength case considered here, the initial ionization rates for the frozen and two-electron models are essentially the same. The potential that the active electron sees in the frozen calculations does not change during ionization so that we find an exponential decay of the probability as expected. The only way the orbital energy in this case can change significantly is if the wave function becomes excited without being ionized. Then the magnitude of orbital energy decreases instead of increasing as in the two-electron case. We find it changes by less than 0.1 eV during this calculation. We show the time-dependent norm of the wave function and projection onto the initial orbital in Fig. 11 for the peak intensity 2×10^{15} W/cm^2. Here again, the projections were taken eight times during each laser oscillation period. In this figure we have plotted the probabilities on a semilog scale to show the exponential decay of the initial state during the constant-intensity period, the last half of the calculation. From the slope of this line, the decay rate can be determined.

In the TDHF calculation, the ionization rate decreases as a function of time due to the weakening of the Coulomb repulsion as the wave-function norm decreases. Therefore, it is difficult to obtain an ionization rate from the decay of the time-dependent norm. However, by plotting the decay rate as a function of the orbital energy at times when $\sin(\omega t)$ vanishes, we find that the ionization rate decreases exponentially with orbital energy, as shown in Fig. 12. Figure 6 shows that the orbital energy has begun to decrease before the intensity has reached its maximum and is approximately -26 eV at the beginning of the constant-intensity interval. From that point on, the log of the rate decreases linearly with increasing orbital energy. The ionization rate for the static Hartree-Fock ground state is obtained by extrapolating the linear falloff back to the correct orbital energy. This rate is compared to the frozen, one-electron results in Table I for several wavelengths and peak intensities. In the long-wavelength regime, we find excellent agreement between the frozen and TDHF results. This presumably implies that ionization requiring many photons which are far from resonant depends weakly on the potential which the electron sees. This also means that theories of multiphoton, multiple ionization which are based on independent electron models should be reasonably successful in the long-wavelength limit. The statistical model of Crance[20,21] and Geltman,[22] for example,

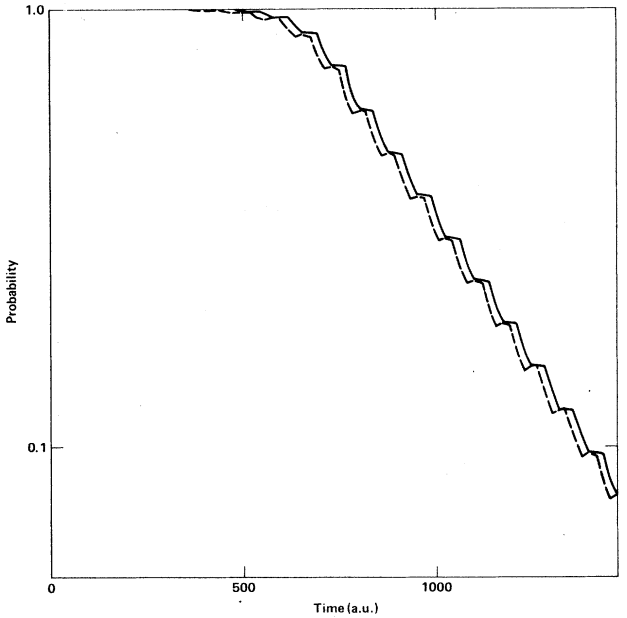

FIG. 11. Time-dependent norm of the one-electron calculation (solid line) along with the ground-state probability corresponding to the case of Fig. 8 but with a peak intensity of 2×10^{15} W/cm^2.

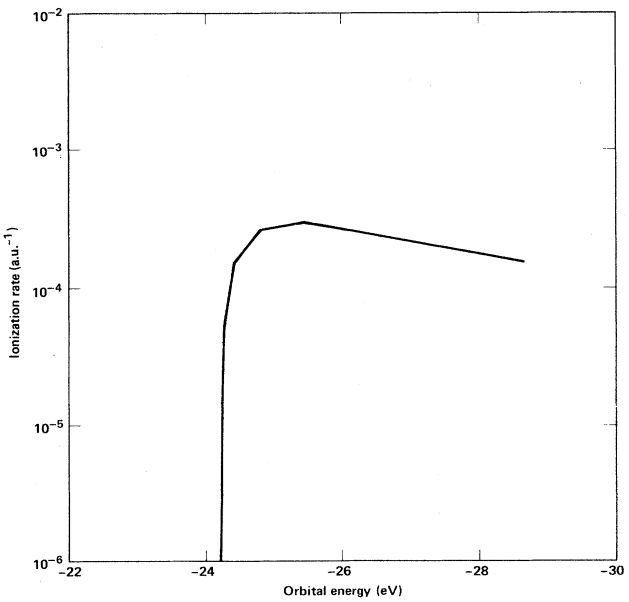

FIG. 12. Helium ionization rate vs orbital energy for 1.064-μm photons and a maximum intensity of 1×10^{15} W/cm^2.

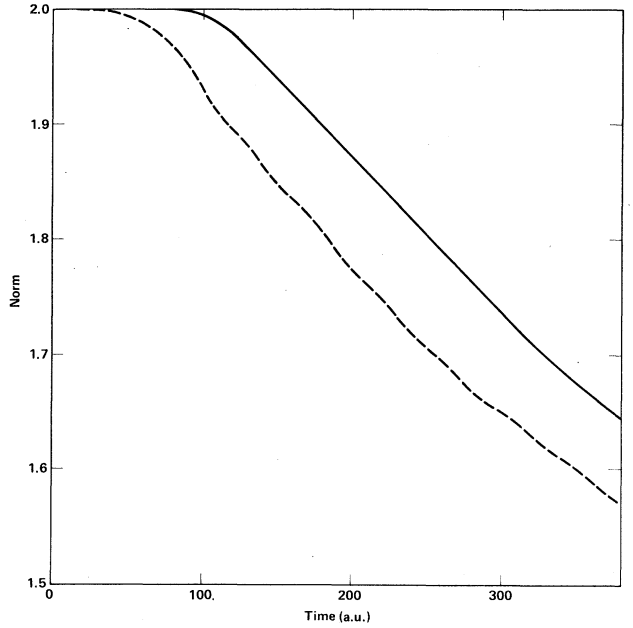

FIG. 13. One-electron calculation of helium ionization by 9-eV photons at $I=1\times10^{15}$ W/cm^2. Solid line is the time-dependent norm and the dashed line is the projection onto the initial state.

seem to work well for Xe with 1.064- and 0.532-μm photons for a large range of intensities.

The photoionization of helium with 9-eV photons has been studied also. This wavelength is also far enough from resonance that direct ionization dominates. Figures 13 and 14 compare the single-electron and TDHF ionization probabilities for laser intensities of 1×10^{15} W/cm^2. In these figures and those that follow, we perform projections and evaluate expectation values only at times when the electric field vanishes [$\sin(\omega t)=0$]. The smooth curves in the figures result from straight-line segments joining the calculated values. The frozen calculation looks similar to the longer wavelength results in that the excitation seems to go directly from the ground state to the continuum. The delay time between the disappearance from the initial state and absorption at the boundary is consistent with the transit time of a few-eV electron. This indicates that the three-photon process is large with probably little contribution from ATI. The TDHF result at early times agrees reasonably well with the single-electron calculations except for a slightly slower decay rate. At long times, it differs significantly. As above, the ionization causes an increase in the magnitude of the orbital energy so that finally the laser wavelength comes into resonance with some transition, presumably three-photon excitation of a Rydberg state, causing, at the latest times shown, Rabi oscillations in the initial-state probability. Figure 15 shows the time dependence of the orbital energy and Fig. 16 the ionization rate versus the orbital energy. The complicated behavior of the latter curve is due to the changing positions of the excited-state energies with the weakening of the Coulomb repulsion. Thus, this single calculation really illustrates the transition from the long-wavelength to the short-wavelength photoionization character. As we discuss below, at shorter wavelengths the resonant transitions in the atom play a strong pole in the excitation dynamics, generally resulting in nonexponential decay of the atom.

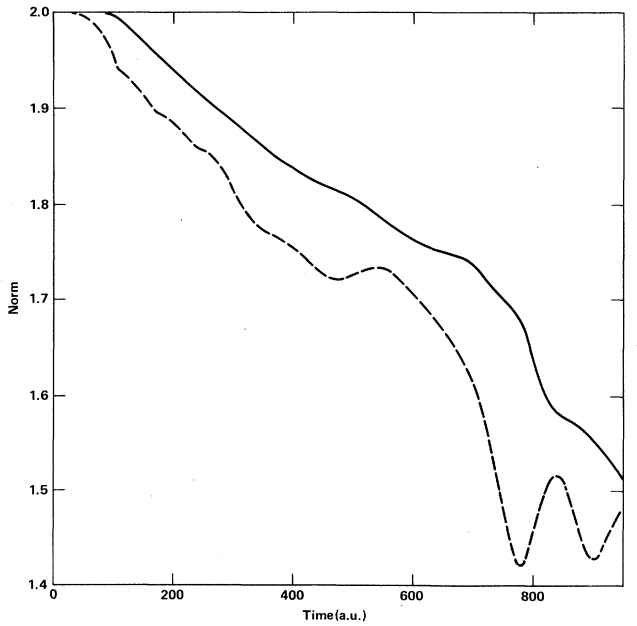

FIG. 14. Same as Fig. 13 but for TDHF calculation. Fifty periods of the field oscillation are shown. Full intensity is reached after five periods.

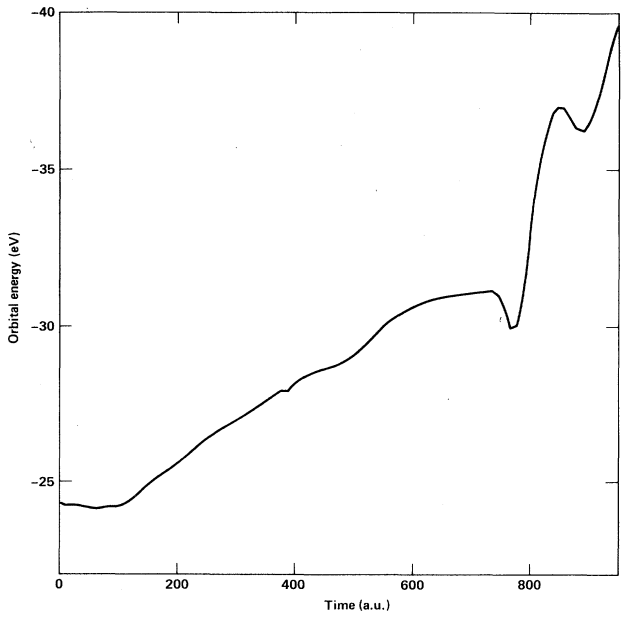

FIG. 15. Orbital energy as a function of time for 9-eV photons at an intensity of 1×10^{15} W/cm^2.

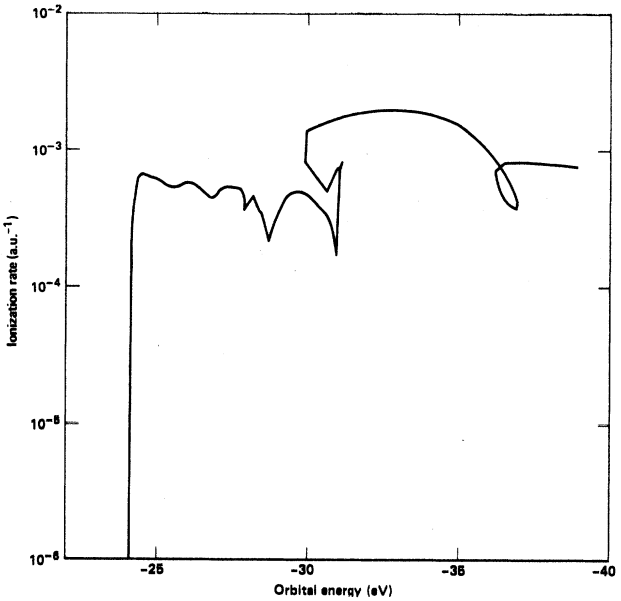

FIG. 16. Ionization rate as a "function" of orbital energy for 9-eV photons at an intensity of 1×10^{15} W/cm^2.

The behavior shown in Fig. 14 can be characteristic of the TDHF method as we have described it. We attempted to clarify our understanding of this result by performing a renormalized (RTHDF) calculation. In this case, after each integration step, we normalize the wave function so that the nonlinearity in the formulation, coupled with the absorbing boundaries, does not produce unrealistic dynamics. Thus we simply multiply our time evolving orbital after each step by a constant, then determine the ionization rate from the magnitude of the renormalization factor averaged over a laser period. In this way we find that the RTDHF 9-eV photoionization rate, shown in Fig. 17, agrees well with the single-electron result and no significant PD occurs. The ionization remains direct and the orbital energy changes by less than 0.2 eV during this calculation. RTDHF calculations of ionization rates for the longer wavelength cases discussed above agree exactly with the extrapolated rates shown in Table I.

The final case we discuss in detail is a short-wavelength case in which the chosen photon energy, 28 eV, exceeds the single-ionization threshold. It is also off resonance for the two-photon excitation of the $2p^2$ doubly excited states which lie near 60 eV in the absence of the field. Again for this case we performed the frozen and TDHF calculations. We note that we performed similar calculations at 30 eV with qualitatively the same results as discussed here.

Figure 18 shows the time dependence of the wave-function norm and its overlaps on the initial $1s$ orbital (short-dashed line) and a $2p$ orbital (long-dashed line). The $2p$ orbital is a single Slater function with an exponential parameter chosen to approximate a $2p^2$ excited state. The intensity reaches its peak after approximately 30 time units then is constant over 35 laser oscillation periods. This calculation was actually done using the RTDHF which arguably gives a more accurate picture of the PD for this two-electron system. A calculation without renormalization for this wavelength is very simi-

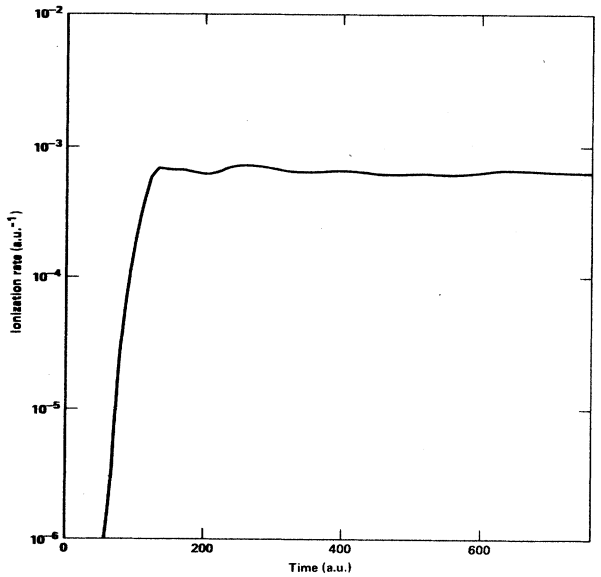

FIG. 17. Ionization rate as a function of time for 9-eV photons at an intensity of 1×10^{15} W/cm^2 from the RTDHF calculation.

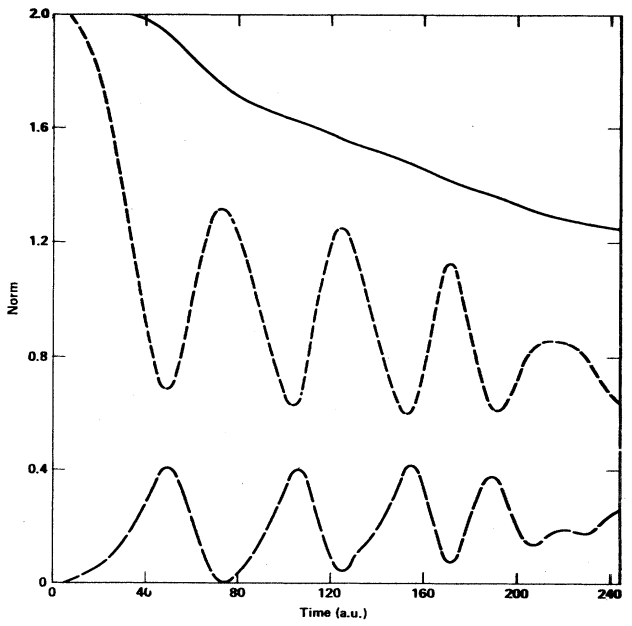

FIG. 18. Wave function norm (solid line) and orbital projections on the $1s$ (short-dashed line) and $2p$ (long-dashed line) as functions of time for the 28-eV photon at a peak intensity of 1×10^{15} W/cm^2.

lar, mainly because the ionization potential does not increase due to the excitation dynamics. This is shown in Fig. 19 where the time dependence of the Coulomb repulsion and kinetic energies are also displayed. Figure 20 shows the time dependence of the nuclear attraction and total energy. These results are to be contrasted to those for the long-wavelength case shown in Figs. 6 and 7. The short-wavelength PD shows a strong excitation of Rabi oscillations between the initial state and some excited state which seems to be $1snp$ and np^2 in character. The fact that we did not optimize the exponential parameters in the p orbital onto which we performed the projection means the precise characterization of the excited state is not possible. However, it is not obvious that a single additional configuration is adequate because of the nonlinear equation which the TDHF wave function obeys. The frozen, single-electron result for this case shows no oscillatory structure. The decay of the initial state falls on top of the dashed curve in Fig. 18 up to about 50 a.u. then continues to decay with a constant rate. Therefore, we conclude that a multielectron process leads to a significant reduction in the ionization rate. Although the laser is well off resonance for any single excitation, the self-consistent potential of the multielectron state is distorted enough by the laser field that a bound (or quasibound) state exists to which reversible excitation from the ground state can occur. The presence of several Rabi oscillations, which eventually appear to be damped, implies the ionization is delayed due to the collective excitation of the electrons. From Fig. 20 we see that up to 40 eV of excitation, well above the ionization threshold, occurs without appreciable loss to the continuum. If the behavior occurs in atoms with many more electrons in the outer shell, a significant amount of energy could be trapped in the atom before ionization. This kind of PD has been postulated by Rhodes and co-workers[6] in discussing their multiple ionization results using high-power uv lasers.

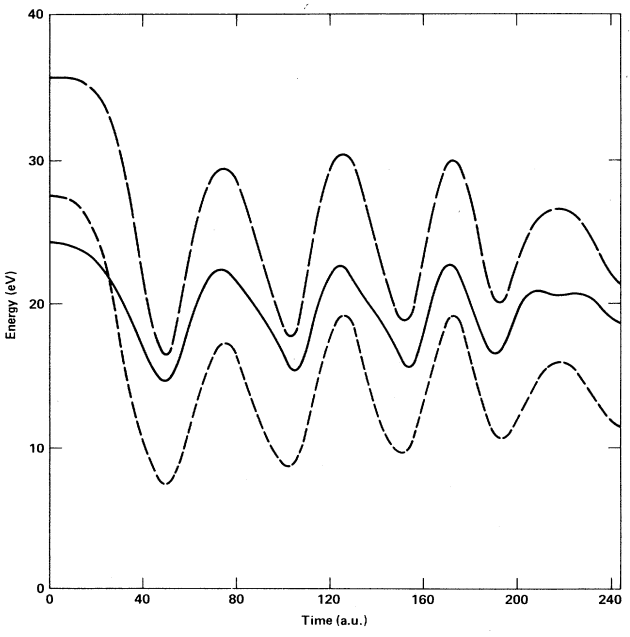

FIG. 19. Time-dependent ionization potential (solid line), Coulomb repulsion (short-dashed line) and single-particle kinetic energy (long-dashed line) for 28-eV photons at an intensity of 1×10^{15} W/cm^2.

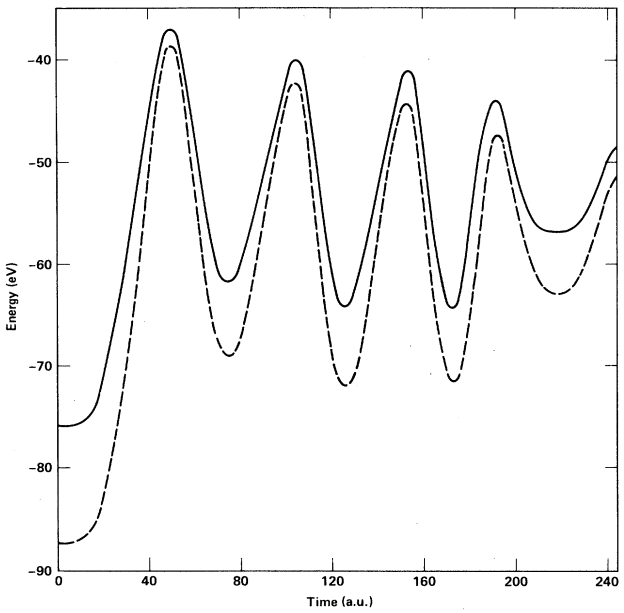

FIG. 20. Time dependence of the total energy (solid line) and nuclear attraction (dashed line) for 28-eV photons at an intensity of 1×10^{15} W/cm^2.

The predicted delay in ionization is on the order of many oscillations of the field (a few fs), so that it would be observable only in *very*-short-pulse-length laser experiments unless some other mode of decay is accessible. Having trapped a large amount of energy in a collective excitation, the atom can relax in several ways: photon emission with a wavelength much shorter than the exciting laser, single or multiple autoionization and core excitation. These modes of decay may not be independent. The possibility of the collective PD, which is indicated by this model, is therefore of great interest as an effect of very intense, short-pulse lasers on multielectron atoms.

Finally, we performed calculations with both long and short wavelengths for a peak intensity of 10^{17} W/cm^2. We find that before the intensity maximum is reached, less than a tenth of a percent of the initial wave function remains on the grid. At this intensity, the numerical TDHF method becomes intractable for the longer wavelengths because of the extended jitter motion of the free electron. For shorter wavelengths the ionization dynamics should be very well represented by the TDHF model as the dominant interaction is with the field. In this case, the ionization rate is so rapid that multiple excitations are not significant. We conclude, therefore, that there could be a window in intensity for which collective modes might be expected.

For lower intensities than those considered in this work, perturbation theory is valid and this type of multiple excitation would be unlikely to play a significant role in affecting the ionization rate. However, a recent paper by Tang and Lambropoulos[23] does show that double excitations can play an important role in ionization dynamics at intensities beyond the range of perturbation theory. In the high intensity, nonperturbative regime, collective excitations may be possible as long as the field is not so high that appreciable ionization occurs within a single oscillation. If excitation-ionization is that rapid, the PD cannot be particularly sensitive to wavelength and it seems unlikely that a collective mode could be established.

IV. CONCLUSIONS

We have presented results of calculations of intense field ionization of helium for a number of laser wavelengths and field strengths. The time-dependent Hartree-Fock method was used to obtain these results. We find limits to the validity or feasibility of this method. For low intensities, such that the rate of excitation is very small compared to our integration times, the method is impractical. Therefore we need to consider intensities which result in ionization rates of at least 10^{11}/s. For 0.532 μm and 1×10^{14} W/cm^2, we found that no excitation occurred within the numerical accuracy of this calculation for any integration time. This should be compared with the observed saturation intensity of 2×10^{13} W/cm^2 for a 50 ps pulse[24] corresponding to an ionization rate on the order of 10^{10}/s. For high intensities and long wavelengths, we found the required grid sizes were unmanageably large due presumably to ponderomotive effects. However, for a significant range of photon energies and intensities, the calculations provide informative and reliable results.

The ionization dynamics were found to be qualitatively different for the short-wavelength versus the long-wavelength regimes. In the former case, the structure of the atomic energy levels was probed and an excitation of a highly energetic doubly excited state was found. Rabi oscillation between this quasibound state and the ground state inhibited the direct ionization process. It may be that this is an artifact of the TDHF model, but if not, it is very encouraging with respect to the possibility observing collective excitations of atoms by strong, short-pulse, short-wavelength lasers. At lower intensities, the doubly excited state is not expected to play a role. Direct ionization should dominate as predicted by perturbation theory. As the intensity increased, a point was reached where appreciable ionization was found to occur during each oscillation of the field. This was found as the peak intensities approached 10^{17} W/cm^2. It is one of the advantages of this method that the strongly nonperturbative regime can be studied for an arbitrary pulse shape. Our calculations predict, then, that there may be a window of intensities for short wavelengths within which collective excitations could be possible.

The long-wavelength regime was investigated both using the TDHF method and a frozen, one-electron model. We found the ionization rate was the same in both cases for the intensity regime studied. In this range of intensities, the ionization rates were found to be nonperturbative in that the order of the process was much less than that given by the minimum number of photons required by the ionization energy. Also the rates were found to become less dependent on wavelength at the highest intensity. We found some evidence of reflections due to the ponderomotive barrier and a consequent slight reduction in the ionization rate. A future communication will deal more thoroughly with this phenomenon. We also concluded that there is likely ATI in the longest wavelength results because of the short delay time between the electron probability leaving the ground state of the atom and being absorbed at the boundary.

The TDHF model produced a changing ionization potential due to the nonlinearity in the Coulomb term. Because of this we discovered an exponential dependence of the ionization rate on the orbital energy. The Keldysh[16] model also predicts an exponential relationship between the ionization potential I_p and the ionization rate. However, this tunneling model contains an extra factor of $I_p^{1/2}$ in the exponent. The PD for the long-wavelength case are uninteresting up until the ponderomotive barrier becomes significant. Up to this point the ionization is direct. At the longest wavelength and highest intensities we considered, the effects of the ponderomotive barrier were not treated correctly because of the limited size of our grid. The rates reported in these cases are expected to be upper bounds on the true rate because the excited flux was absorbed at our boundary before it could be reflected by the barrier. We determined the effect was on the order of 15% for the 532-nm photons at 1×10^{15} W/cm^2, but may be higher in other cases. This effect places an upper bound on the wavelenghs we can consider for a given intensity. The trapping of excited electrons by this barrier is a second mechanism for collective excitation in the atom. Time-dependent calculations can provide new insight into the length of the trapping time and therefore the importance of this effect.

The angular distribution of emitted electrons was found to differ strongly with wavelength. The longest wavelength results were most strongly collimated along the direction of polarization as has been found in experiments on xenon.[5]

Finally, our calculations allowed the variation of the intensity of the laser field with time. For these initial calculations, we considered only cases with wavelengths far from resonance. Therefore little effect due to the duration of the turn-on period was found. Only in the case for which no turn-on period was used [$t_{\max}=0$ in Eq. (10)] was there evidence of some ringing in the excitation dynamics. For wavelengths closer to resonance, the ionization results will be much more sensitive to the pulse shape.

The pulse lengths over which interesting dynamics and possible collective effects are expected to be important are short compared to those used in most experiments to date. Long-pulse experiments suffer from rapid ionization during the rise time of the pulse, so that the neutral atom may never experience the peak intensity.[8]

If the pulse time can be reduced to tens of oscillation periods (<50 fs), then it should be possible to study the PD in detail.

The TDHF model of multiphoton ionization has produced may interesting results regarding PD. One might ask about the effects of relaxing the single configuration constraint to consider, for example, an unrestricted Hartree-Fock–type initial state,

$$\Psi(12)\doteq\phi_{1s}(1)\phi_{1s'}(2)+\phi_{1s'}(1)\phi_{1s}(2)\ . \tag{14}$$

In this case each electron will move independently in the average field of the other. Our calculations show that for the long-wavelength case, this change will not significantly affect the ionization dynamics which were found to be direct and insensitive to the excited states of the atom. For shorter wavelengths, and intensities not so high that the interelectronic interactions are relatively weak compared to the field, this relaxation of the orbital constraint should be very important. It will allow much more accurate representation of the excited states, allow autoionization, and include the relaxation of one of the orbitals to the more compact $He^+(1s)$ state. Such a generalization of the procedure used here is presently under way and will produce more definitive information about the role of collective excitations in multiphoton ionization.

ACKNOWLEDGMENTS

The author wishes to thank Dr. Charles Cerjan and Dr. Bruce Shore for many useful discussions concerning the interpretation of the results presented here. This work was performed under the auspices of the Department of Energy at Lawrence Livermore National Laboratory, Livermore, California, under Contract No. W-7405-Eng-48.

[1]P. Agostini, F. Fabre, G. Mainfray, G. Petite, and N. K. Rahman, Phys. Rev. Lett. **42**, 1127 (1979).
[2]P. Kruit, J. Kimman, and M. J. van der Wiel, J. Phys. B **14**, L597 (1981).
[3]R. R. Freeman, T. J. McIlrath, P. H. Bucksbaum, and M. Bashkansky, Phys. Rev. Lett. **57**, 3156 (1986).
[4]A. L'Huillier, L.-A. Lompre, G. Mainfray, and C. Manus, Phys. Rev. Lett. **48**, 1814 (1982).
[5]T. S. Luk, H. Pummer, K. Boyer, M. Shakidi, H. Egger, and C. K. Rhodes, Phys. Rev. Lett. **51**, 110 (1983).
[6]T. S. Luk, V. Johann, H. Egger, H. Pummer, and C. K. Rhodes, Phys. Rev. A **32**, 214 (1985).
[7]*Multiphoton Ionization of Atoms,* edited by S. L. Chin and P. Lambropoulos (Academic, Orlando, 1984).
[8]P. Lambropoulos, Phys. Rev. Lett. **55**, 2141 (1985).
[9]K. C. Kulander, Phys. Rev. A **35**, 445 (1987).
[10]K. R. Sandhya Devi and S. E. Koonin, Phys. Rev. Lett. **43**, 512 (1981).
[11]K. C. Kulander, K. R. Sandhya Devi, and S. E. Koonin, Phys. Rev. A **25**, 2968 (1982).
[12]K. R. Sandhya Devi and J. D. Garcia, Phys. Rev. A **30**, 600 (1984).
[13]S. E. Koonin, K. T. R. Davies, V. Maruhn-Rezwani, H. Feldmeier, S. J. Krieger, and J. W. Negele, Phys. Rev. C **15**, 1359 (1977).
[14]T. W. B. Kibble, Phys. Rev. **150**, 1060 (1966).
[15]J. H. Eberly, Prog. Opt. **7**, 359 (1969).
[16]M. H. Mittleman, *Introduction to the Theory of Laser Atom Interactions* (Plenum, New York, 1982).
[17]L. V. Keldysh, Zh. Eksp. Teor. Fiz. **47**, 1945 (1964) [Sov. Phys.—JETP **20**, 1307 (1965)].
[18]N. B. Delone, B. A. Zon, and V. P. Krainov, Zh. Eksp. Teor. Fiz. **75**, 445 (1978) [Sov. Phys.—JETP **48**, 223 (1978)].
[19]A. Szöke and C. K. Rhodes, Phys. Rev. Lett. **56**, 720 (1986).
[20]M. Crance, J. Phys. B: At. Mol. Phys. **17**, 4323 (1984).
[21]M. Crance, J. Phys. B: At. Mol. Phys. **18**, L155 (1985).
[22]S. Geltman, Phys. Rev. Lett. **54**, 1909 (1985).
[23]X. Tang and P. Lambropoulos, Phys. Rev. Lett. **58**, 108 (1987).
[24]L.-A. Lompre, A. L'Huillier, G. Mainfray, and C. Manus, Phys. Lett. **112A**, 319 (1985).
[25]G. A. Victor, Proc. Phys. Soc. **91**, 825 (1967).
[26]B. Ritchie, Phys. Rev. A **16**, 2080 (1977).
[27]A. L'Huillier, L. Jönsson, and G. Wendin, Phys. Rev. A **33**, 3938 (1986).
[28]J. W. Cooper, Phys. Rev. **128**, 681 (1962).